

Iranian Journal of Oil & Gas Science and Technology, Vol. 10 (2021), No. 2, pp. 63–89
<http://ijogst.put.ac.ir>

Preparation of Nickel Oxide Supported Zeolite Catalyst (NiO/Na-ZSm-5) for Asphaltene Adsorption: A Kinetic and Thermodynamic Study

Mohsen Mansouri¹, Mehdi Parhiz², Behrouz Bayati³, and Yaser Ahmadi^{1*}

¹ Assistant Professor, Chemical and Petroleum Engineering Department, Ilam University, P.O. Box 69315/516, Ilam, Iran

² M.S. Student, Chemical and Petroleum Engineering Department, Ilam University, P.O. Box 69315/516, Ilam, Iran

³ Associate Professor, Chemical Engineering Department, Faculty of Engineering, Ilam University, Ilam, Iran

Highlights

- Using NiO/Na-ZSm-5 for solving the asphaltene precipitation problem;
- Performing asphaltene adsorption experiments at various asphaltene concentrations, temperatures, and ratios of heptane to toluene;
- Determining the kinetic mechanisms according to the pseudo-first-order and pseudo-second-order models;
- Evaluating the thermodynamic conditions and the spontaneity of the asphaltene adsorption process.

Received: November 17, 2020; revised: January 28, 2021; accepted: March 04, 2021

Abstract

One of the critical issues in the oil industry is related to asphaltene precipitation during different stages, and using nanoparticles is known as a standard method for solving this problem. Although nickel oxide and zeolite have been addressed in previous research to solve the asphaltene precipitation problem, using NiO/Na-ZSm-5 (the primary goal of this study) has not been developed to solve relevant asphaltene precipitation problems. The crystalline structure and morphology of the synthesized nanoparticles were analyzed with the help of X-ray diffraction spectrometry (XRD), scanning electron microscopy (SEM), Fourier transform infrared spectroscopy (FTIR), and energy-dispersive X-ray spectroscopy (EDXS). The results show that the nanoparticles were well synthesized and preserved their crystalline structure with a diameter of 13.6 nm after synthesis. The EDXS analyses also proved that the sorbent adsorbed an amount of asphaltene. In the next step, asphaltene adsorption experiments were carried out at various concentrations of asphaltene and temperatures, and the effect of different variables, including the initial concentration of asphaltene, temperature, and the ratio of heptane to toluene, on the asphaltene adsorption rate was evaluated. The results indicate that with an increase in the initial asphaltene concentration from 25 to 2000 ppm, the asphaltene adsorption rate in zeolite increases. At concentrations less than 500 ppm, a rise in the temperature reduces the asphaltene adsorption, while at concentrations higher than 500 ppm, raising the temperature from 25 to 55 °C increases asphaltene adsorption capacity on zeolite. Further, more significant adsorption is observed at a heptane-to-toluene ratio of 0.4 with $q = 25.17$ mg/g. Evaluating the effects of kinetic adsorption molecules of asphaltene on these nanoparticles shows that the adsorption process reaches equilibrium in less than 2 h. The experimental data were adapted according to Lagrangian pseudo-first-order and pseudo-second-order models to determine the kinetic


* Corresponding author:
Email: yaser.ahmadi@ilam.ac.ir

mechanism of this process. The Langmuir and Freundlich adsorption isotherms were evaluated, and the isotherms resulting from the Langmuir isotherm model were of good conformity, indicating that adsorption at the homogenous level occurred with a single-layered coating. In the final step, after evaluating the thermodynamic conditions, the spontaneity of the asphaltene adsorption process was proved.

Keywords: Adsorption Kinetics; Asphaltene; Nanoparticles; Nickel oxide; Zeolite

How to cite this article

Mansouri M, Parhiz M, Bayati B, Ahmadi Y, Preparation of Nickel Oxide Supported Zeolite Catalyst (NiO/Na-ZSm-5) for Asphaltene Adsorption: A Kinetic and Thermodynamic Study. *Iran J. Oil Gas Sci. Technol.*, Vol. 10, No. 2, pp. 63–89, 2021.

DOI: <http://dx.doi.org/10.22050/IJOGST.2021.257740.1571>, This is an Open Access article under Creative Commons Attribution 4.0 International License.(creativecommons.org/licenses/by/4.0/) 

1. Introduction

Nowadays, the hydrocarbon industry encompasses a significant part of the world economy and is the primary energy source. Therefore, optimizing processes and solving problems related to the oil industry have been of interest to researchers [Kinitisch et al. 2007]. The fraction of asphaltene available in crude oil has resulted in numerous problems in oil industries such as mining, transportation, reserves, and refinement [Novaki et al. 2016]. Flocculation and precipitation of asphaltene have resulted in reduced extraction capacity from crude oil sectors, and this reduced efficiency is due to the obstruction of pipelines and various equipment parts [Novaki et al. 2016, Zhang et al. 2007, Belal et al. 2012].

Asphaltene is defined based on the solubility model; while they are insoluble in paraffin solutions such as heptane and normal pentane, they are soluble in aromatic solutions such as benzene and toluene [Bouhadda et al. 2007]. In addition to hydrogen and carbon, asphaltene molecules have heteroatoms such as nitrogen, oxygen, sulfur, and a small number of other metals such as vanadium, iron, and nickel, which result in sedimentation of asphaltene [Groenzin et al. 2000, Kralova et al. 2011, Hemmati-Sarapardeh et al. 2013, Rudyk et al. 2014]. Numerous studies have confirmed that metal and polar asphaltene (especially vanadium) cause the most significant solubility problems [Nassar et al. 2015].

Due to thermodynamic instability, asphaltene is initially found as suspended nuclei of sediments, and then with further instability and passage of time, it will experience a growth and adhesion phenomenon. Finally, as the particles grow, whereas the liquid environment will not have the ability to suspend them, precipitation occurs in the asphaltene particles [Escobedo et al. 2010, Ferworn et al. 2010, Mullins et al. 2007, Khoshandam et al. 2010]. The thermodynamic instability factors for asphaltene precipitation can be changes in pressure, temperature, or a combination of crude oil, resulting in asphaltene precipitation as a solid phase [Östlund et al. 2004].

One of the effective methods for controlling asphaltene precipitation is using chemical additives such as surfactants [Raj et al. 2019] and nano-adsorbents. During the past few years, nanotechnology has played an essential role in the oil industry, significantly enhancing oil recovery [Bahraminejad et al. 2019, Eslahati. 2020, Mehrabianfar. 2021, Nowrouzi. 2020, Nazarahari et al. 2020] and catalytic behavior [Medina et al. 2019, Marei et al. 2019], making it an excellent choice for adsorption and decomposition of asphaltene.

Among the nano-adsorbents, zeolites are considered the most reliable adsorbents due to their particular pores, cage-like structure, and appropriate thermal stability. Zeolites are alumina silicate hydrated minerals with a very fine structure [Kosinov et al. 2018]. Due to the stability, large surface area, and

orderliness of the pore structure, zeolites have numerous applications in catalyst processes [He et al. 2018, Fakeeha et al. 2013]. Another advantage of zeolites is their ability to separate metal atoms and prevent the closure of metal atoms. Among various zeolites, ZSM-5 is a high adsorption potential due to its physical features and unique shape [de Oliveira et al. 2018]. Research shows that oxygen and nitrogen are essential factors in asphaltene adsorption in nanoparticles, whereas higher nitrogen increases asphaltene adsorption. This is while sulfur has a negative effect on asphaltene adsorption [Nassar et al. 2011, Camilo et al. 2013, Gonzalez, 2007, Nassar, 2012]. In addition, it has been specified that other factors such as the amount of water and the H/C ratio or aromatic rings affect the asphaltene adsorption capacity [Nassar et al. 2011, Camilo et al. 2013]. Asphaltene adsorption also depends on the asphaltene structure, amount of resin, the polarity of solvents, temperature, and contact time [McLean. 1997, Simo. 2007]. Some sources have considered temperature a facilitator in forming asphaltene precipitation, while others consider temperature an inhibitor in forming the asphaltene solid phase [Hasanvand et al. 2015, Tavakkoli. 2014, Leontaritis et al. 1987]. In this research, the effects of different temperatures and variables such as the initial concentration of asphaltene and the ratio of heptane to toluene (H/T) were thoroughly addressed in the presence of prepared nanoparticles.

Nanoparticles with a unique average surface have higher adsorption. It is observed that the adsorption process is not uniform and occurs at a specific level. Recently, nanoparticle synthesis of nickel oxide and the use of these particles for asphaltene adsorption from asphaltene–toluene solution has been the focus of attention in experimental studies [Tu et al. 2006]. The results indicate that increasing nickel nanoparticles in the alumina nano adsorption structure increases asphaltene adsorption of the toluene solution [Camilo et al. 2013]. Among the nickel features as adsorbent, the effect of temperature on adsorption can be referred to, whereas a higher temperature will result in a considerable increase in asphaltene adsorption. In addition, nickel promotes the formation of multiple layers, which justifies the more significant adsorption of asphaltene [Ma et al. 2005]. In the research conducted by Franco et al. on alumina nanoparticles, it was specified that increasing the amount of nickel in the nanoparticle from 5% to 15% has a significant effect on asphaltene adsorption [Ma et al. 2005]. Moreover, in another experiment, asphaltene adsorption on the silica gel nanoparticle with 5% and 15% nickel oxide was evaluated, which showed that higher nickel amounts improved asphaltene adsorption on the nanoparticle [Cortés et al. 2012].

Many researchers use NiO and other nanoparticles. It was specified that in the presence of nanoparticles, the asphaltene agglomeration became smaller. Furthermore, these nanoparticles had high potential in the aspect of asphaltene adsorption on their surface, as listed in Table 1. In this research, using NiO/Na-ZSm-5 is developed for the possible investigation of solving asphaltene precipitation which is not developed among researchers according to our knowledge.

Table 1
Using NiO and other nanoparticles for asphaltene adsorption.

Results	Material	Year	Reference
The nanoparticle synthesis method and their final properties affect asphaltene adsorption, demonstrating that synthetic nano nickel oxide has 15% less adsorption than commercial nano oxide.	NiO	2012	[Belal et al. 2012]
Oxide nanoparticles have a higher adsorption capacity, and nanoparticles prepared on the spot have an adsorption capacity of 2.8 g asphaltene per gram of nanoparticle.	NiO	2012	[Belal et al. 2012]
An increase in nickel nanoparticles results in increased asphaltene adsorption.	NiO	2013	[Camilo et al., 2013]

Results	Material	Year	Reference
An increase in the amount of nickel in the nanoparticle has a considerable effect on asphaltene adsorption.	Al ₂ O ₃ and NiO	2013	[Camilo et al., 2013]
A more significant amount of nickel results in enhanced asphaltene adsorption on the nanoparticle.	SiO ₂ and NiO	2012	[Cortés et al. 2012]
In the presence of nanoparticles, the size of asphaltene aggregates becomes smaller while their number increases.	NiO, SiO ₂ , and Fe ₃ O ₄	2018	[Li et al. 2018]
An increase in the amount of heptane in the solvent containing nanoparticles results in increased adsorption.	NiO, SiO ₂ , and Fe ₃ O ₄	2015	[Kazemzadeh et al. 2015]
Metal oxide nanoparticles have a significant effect on the thermal decomposition of heavyweight hydrocarbons such as asphaltene, and among the nanoparticles evaluated, nickel oxide has the highest adsorption capacity.	NiO, CO ₃ O ₄ , and Fe ₃ O ₄	2011	[Nassar et al. 2011]
Among the nanoparticles evaluated for asphaltene adsorption, nickel oxide has a higher adsorption capacity compared to the other adsorbents.	NiO, Fe ₂ O ₃ , WO ₃ , Mn ₂ O ₃ , CuO, silica, and Co ₃ O ₄	2014	[Hosseinpour et al. 2014]
In the evaluation of uncoated nanoparticles, it was found that nickel oxide has the highest adsorption capacity.	NiO, Fe ₂ O ₃ , WO ₃ , ZrO ₂ , fumed silica, CaO, CeO ₂ , MgO, and CaCO ₃	2013	[Hosseinpour et al. 2013]
All adsorbents follow the Langmuir isotherm and have single-layer adsorption. Nickel oxide also has higher adsorption than the other two adsorbents at all temperatures.	NiO, MgO, and Fe ₃ O ₄	2019	[Kashefi et al. 2018]

Due to its low cost, availability, and physical and chemical characteristics, nickel oxide is an acceptable option for catalytic processes. In this study, the NiO/Na-ZSm-5 catalyst was used to remove asphaltene for the first time. Therefore, due to the high adsorption of nickel oxide, this catalyst was evaluated as a new adsorbent for asphaltene precipitation, enhancing the extraction efficiency. Asphaltene adsorption on solid surfaces is usually proposed by Langmuir and Freundlich models, expressing single-layer and multilayer adsorption, respectively [Mirzayi et al. 2014, Acevedo et al. 2003]. The results of studies show that single-layer and multilayer adsorption behaviors depend on the asphaltene source used in the laboratory [Acevedo et al. 2003, González et al. 1993, Marczewski et al. 2002, Balabin et al. 2010, Jouault et al. 2009]. Franco et al. studied the kinetic and thermodynamic asphaltene adsorption on stone powder surface tanks at various temperatures and times. According to the results obtained, the Langmuir isotherm model was in good accordance with asphaltene surface adsorption [Acevedo et al. 2000]. Kashefi et al. evaluated NiO, MgO, and Fe₃O₄ adsorbents for asphaltene adsorption in their study. All the adsorbents followed the Langmuir isotherm and had single-layered adsorption. In addition, nickel oxide had higher adsorption compared to the two other adsorbents [Kashefi et al. 2018].

In order to evaluate the kinetic adsorption of asphaltene, two pseudo-first-order and pseudo-second-order models were presented. The study results by Acevedo et al. indicate that asphaltene adsorption on one type of silica gel follows the first-order kinetic model. In such conditions, it can be stated that the adsorption process is better controlled by permeation into the adsorbent surface, permeation to the joint surface, and permeation inside the cavities of porous surfaces [Acevedo et al. 2000]. This study aims to

evaluate the nano-adsorption of Na-ZSM-5 nickel oxide at different temperatures and concentrations and various heptane-to-toluene ratios. The results were evaluated using different adsorption isotherms and kinetic and thermodynamic parameters. Further, the physical and chemical features of the adsorbent were evaluated using X-ray diffraction spectrometry (XRD), scanning electron microscopy (SEM), Fourier transform infrared spectroscopy (FTIR), and energy-dispersive X-ray spectroscopy (EDXS).

2. Experimental procedures

2.1. Materials

Normal heptane obtained from Merck Co. was used with 99% purity for precipitating asphaltene, and toluene with a purity of 96% was obtained from Iran Chemistry Co. for solving it. The nickel oxide catalyst was used as the precipitated asphaltene adsorbent. For catalyst synthesis, nickel nitrate and sodium hydroxide were obtained from Merck and Ghatran Chemical Co., respectively. Table 2 provides the characteristics of the material used in this work.

Table 2
The materials used in this work with their relevant function.

Material	Application
Toluene	Solubilization
N Heptane	Extraction
Zeolite Na-ZSM-5	Sorbent
Nickel Nitrate	Catalyst synthesis
Sodium Hydroxide	Catalyst synthesis

Also, asphaltene filtration paper grade 42" with a pore size of 0.22 μm was used.

2.2. Catalyst synthesis

The co-precipitation method was used to build the nickel oxide–zeolite (Na-ZSM-5) catalyst, for which 20% nickel and 80% zeolite (Na-ZSM-5) were used. For the catalyst synthesis, 10 g of a nickel nitrate salt was initially poured into 100 cc water and stirred for 20 to 30 min. Then, 8 g of ZSM-5 was added and mixed for another 20 min. For preparing ZSM-5, the gel was first prepared by combining the molar percentage of Al_2O_3 :46, SiO_2 : 2.7, TPA: 5, Na_2O : 1.3, Trien: 2500 H_2O and pouring them into a Teflon autoclave chamber so that it fills 70% of its volume. After complete closure and sealing, the autoclave was placed in a temperature-controlled chamber for 72 h. After completing the heat treatment, the autoclave was cooled, and the products were removed. After passing through the strainer, these products were washed with water so that the pH of the solution passing through the strainer was 7.0.

Triethylene tetraamine also acts as a chelating agent in this work. After drying at 100 $^{\circ}\text{C}$ for 12 h, the resulting powder was calcined for 8 h to remove the mold so as to obtain ZSM-5 zeolite powder. The mixer should be at 70 $^{\circ}\text{C}$ and 700 rpm during the entire experiment. Sodium hydroxide was used for catalyst synthesis because it was the least expensive and most widely used alkaline material. Due to its high alkaline quality and economic features, it has been given more significant consideration. Sodium hydroxide (NaOH) was poured into containers and added drop-wise to the solution until reaching a pH of 8.0. After reaching the considered pH, the system was kept in this condition for a maximum of 1 to 2 h until precipitation occurs. The next phase was washing the obtained precipitation with distilled water. After collecting the washed precipitation, it was placed in an oven for 16 h at 120 $^{\circ}\text{C}$. The dried precipitation was removed from the oven, weighed, placed in a crucible, and then put in a furnace at

500 °C for 5–6 h to obtain calcination [Mishra et al. 2012, Rahdar et al. 2015]. Figure 1 shows the simple flowchart of making the nickel oxide–zeolite (Na-ZSM-5) nanoparticles.

2.3. Extracting asphaltene from bitumen using the IP143 method

It is noteworthy that normal paraffin (normal pentane and normal hexane) is a precipitator of asphaltene, and it should be considered that aromatic solvents (toluene, benzene, and hexane) are asphaltene solvents. The method for conducting IP143 is given below [59].

1. Crude oil with a ratio of 40 to 1 is mixed with normal paraffin for precipitating the existing asphaltene, and then the initial reflux is carried out for 1.5 h (for a complete mixture of crude oil and normal paraffin). All the steps mentioned above are carried out for precipitating all the asphaltene in crude oil, even though a small number of other elements in crude oil might precipitate along with asphaltene.
2. The reflux mixture is placed in a dark environment for 24 h so that asphaltene can adequately precipitate (in balloon 1).
3. The mixture is placed inside a funnel and filtered in balloon 2 using filter paper to separate the precipitated asphaltene. Solid asphaltene aggregates onto the filter paper and maltin (aromatic, saturated, and resin) pass through the filter paper and aggregates inside balloon 2. However, some maltin also aggregates onto the paper. Normal paraffin (40 cc) is added to balloon 2, and the secondary reflux is conducted until the filter paper contains only asphaltene (black).
4. At this step, filter paper is situated inside the small part of the bubble column and carries out reflux with balloon 2. This reflux continues until the filter paper has only black-colored particles related to asphaltene.

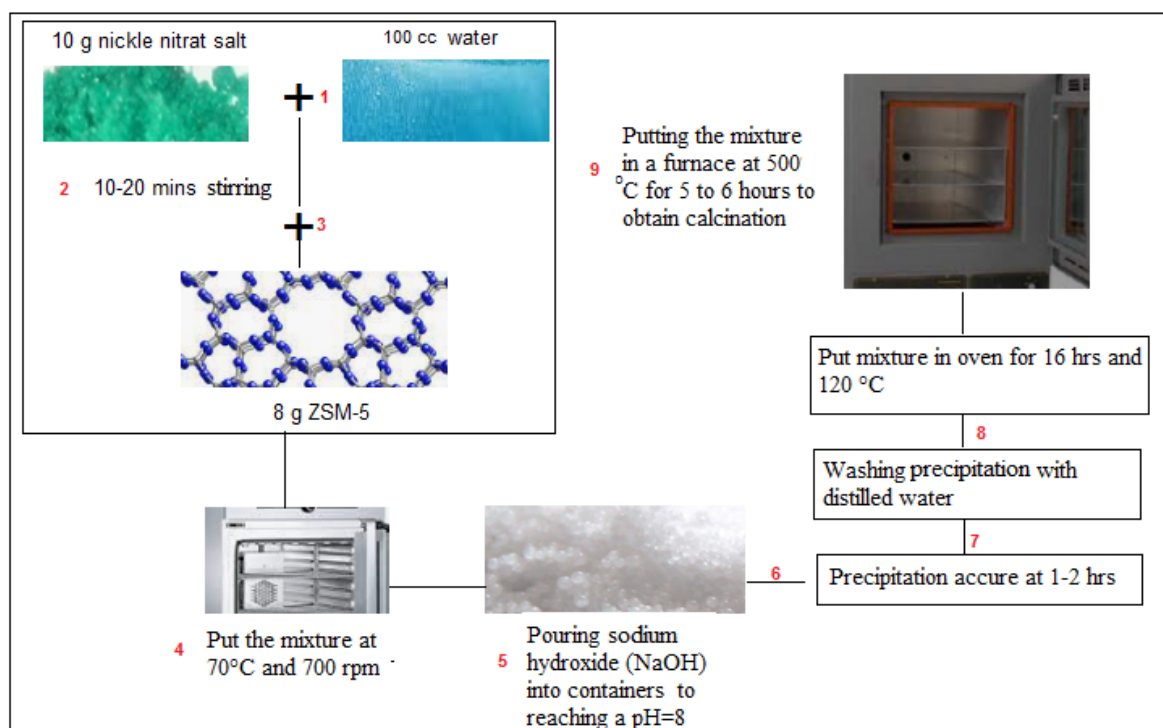


Figure1

The flowchart for the simple chemical route synthesis process of Na-ZSM-5 nanoparticles.

Separating asphaltene adsorbed on filter paper has to be done using a strong solvent. To this end, the filter paper is kept at the small detached part of the bubble column, and 100 cc of toluene is added to balloon 1 with precipitated asphaltene; this balloon is connected to the bubble column reactor, and the

third reflux is continued until the filter paper returns to its original color. Now balloon 1 includes toluene and asphaltene. Due to the volatility of toluene, the material inside balloon 1 is transferred to the beaker, which is placed under the hood for 24 h, and then the mass of the beaker is measured. At time intervals of 6 h, the beaker mass is measured again, and the toluene vaporization process continues under airflow until changes in mass are observed at less than 0.002 g. During this process, toluene evaporates, and dry asphaltene remains at the bottom of the container [Jia et al. 2011]. After the extraction process, an asphaltene reference solution with a concentration of 2000 mg/L is provided inside toluene. This solution is used in the following steps to provide solutions with specific concentrations, plot calibration curves, and conduct adsorption experiments.

2.4. Removing asphaltene with adsorbent

A 200 cc tank of 2000 ppm asphaltene and the solutions including 25, 50, 250, 350, 500, 1000, and 2000 ppm are provided. Experiments began with 42 cc, for which in the UV analysis of 0, prior to pouring the catalyst inside the container, 2 cc of toluene asphaltene solution should be separated, and 8 cc pure toluene should be added. Then, the solution should be poured through a filter and placed in a UV device.

It is noteworthy that for analyzing with the UV device, 2 cc of asphaltene solution should always be used along with 8 cc pure toluene. Now, we have 40 cc of the solution, including asphaltene and toluene. The catalyst (0.4 g) is added to the solution, and this amount of catalyst is equal to 10 g/L, for which sampling is done at 30, 60, 90, 120, and 150 min. Experiments begin when the catalyst is added to a 40 cc solution and is placed at a specific distance and temperature. All the experiments are carried out at 400 rpm, and the samples are analyzed at ambient temperature and a temperature of 40 and 50 °C.

The time intervals are reduced for lower concentrations because the solution reaches equilibrium sooner. The concentration that has reached equilibrium is considered the most significant amount. Hence, the concentration of solutions is measured using a UV–Vis device. Therefore, the equilibrium concentration value (C) of asphaltene can be obtained after adding the catalyst. Equation (1) calculates the asphaltene adsorption capacity over the adsorbent (zeolite Na-ZSM-5 nickel oxide):

$$q = \frac{C_0 - C_t}{m} V \quad (1)$$

where C_0 (mg/L) is the initial concentration of the asphaltene solution, C_t (mg/L) indicates the asphaltene solution concentration at any time, m (g) denotes the weight of nanoparticle used, V (L) is the asphaltene solution volume, and q (mg/g) represents the adsorbent capacity in milligrams of asphaltene over grams of adsorbent [Yudin et al. 1998]. All the experimental conditions are repeated for temperatures of 40 and 55 °C.

3. Results and discussion

3.1. Plotting the calibration curve

Figure 2 shows the UV calibration curve at 25, 40, and 55 °C. To this end, solutions are provided with concentrations of 25–2000 ppm of asphaltene in toluene adsorbent at ambient temperature, 40, and 55 °C, diluted from the more concentrated solution. The asphaltene solution was analyzed using the UV–Vis spectrophotometer to determine the maximum wavelength with different concentrations. A wavelength of 620 nm was determined as the maximum wavelength. After determining the maximum wavelength, solution adsorption rates were obtained for concentrations of 25–2000 ppm using the UV–Vis spectrophotometer at maximum wavelengths, and the curve of adsorption rate was plotted based on concentration. As shown in Figure 2, the calibration curve related to asphaltene solution at ambient

temperature is linear, with a correlation coefficient of 0.998. These conditions are also repeated for a temperature of 40 and 55 °C. A linear diagram and acceptable R^2 are obtained at different temperatures.

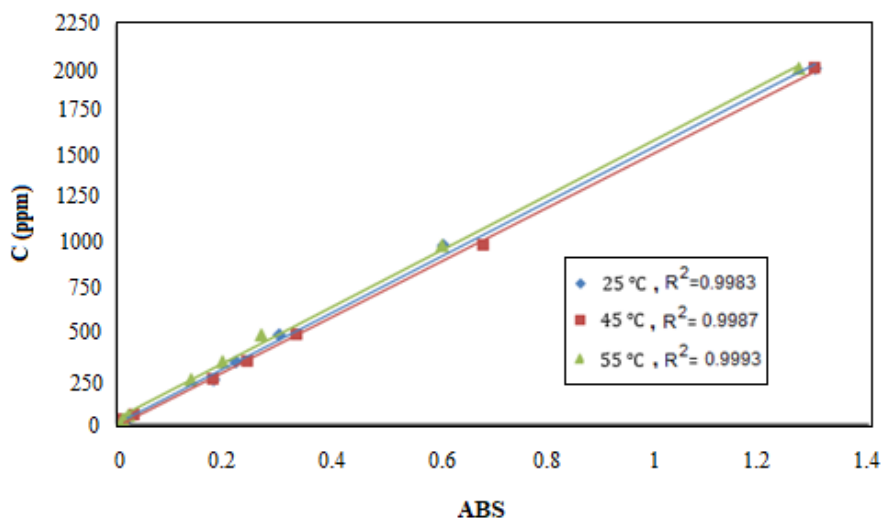


Figure 2

The calibration curves at 25, 40, and 55 °C.

3.2. Analysis of X-ray diffraction

The XRD pattern of Na-ZSM-5 zeolite is shown in Figure 3, and the mixture with zeolite nickel oxide is shown in Figure 4 from 1° to 80°. In addition to determining the crystalline structure of materials, the XRD method can evaluate any structural changes resulting from chemical and physical effects on the material. The peaks in Figure 3 are compatible with previous research [Charchi Aghdam et al. 2019, Ziebro et al. 2010]. The peaks at a 2θ of 7.5°, 8.5°, 23°, and 24° confirm Na-ZSM-5 zeolite while preserving the crystalline structure of zeolite after synthesis [Sedighi et al. 2018]. Moreover, the intensity of peaks shows the high crystallinity of zeolite [Shams-Ghahfarokhi et al. 2015, Qiao et al. 2009]. The peak at a 2θ of 30° is related to the crystalline phase of quartz with a cubic structure [65]. In addition, the peaks at a 2θ of 29.12°, 39°, 42°, and 63° demonstrate nickel oxide (NiO) in a catalyst structure [Qiao et al. 2009, Dong et al. 2019, Hashem et al. 2016, Milovanović et al. 2016, Londoño-Calderón et al. 2020].

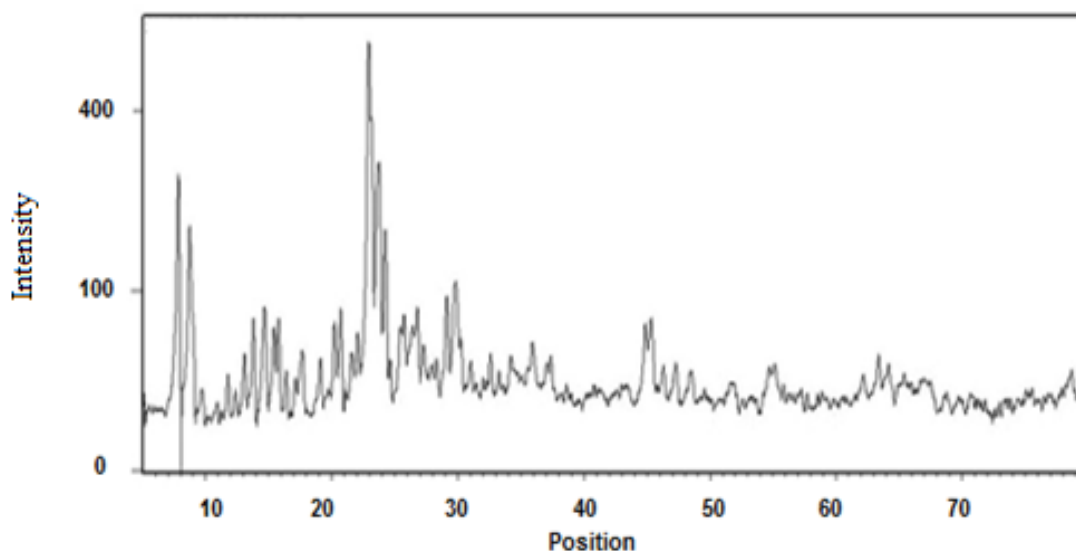


Figure 3
The XRD pattern of the Na-ZSM-5 zeolite.

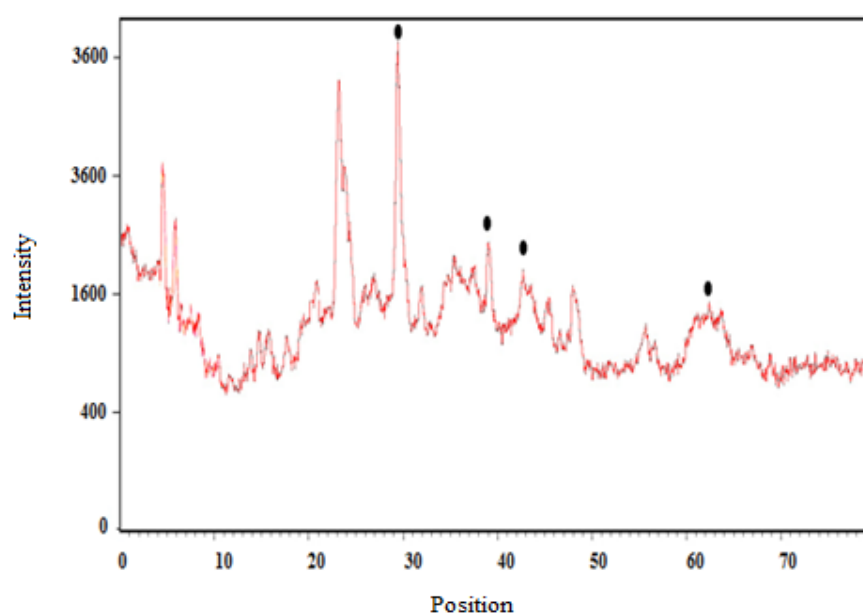


Figure 4
The XRD pattern of the NiO-Na-ZSM-5 zeolite.

3.3. Infrared spectroscopy

FTIR tests are depicted in Figure 5 for nickel oxide zeolite Na-ZSM-5. Peaks at 540, 790, 1085, 1634, and 3361 cm^{-1} have good conformity to zeolite adsorption [Ziebro et al. 2013]. All zeolites have a high peak near the wavelength of 3445 cm^{-1} , which is the siloxane or hydroxyl groups of water adsorbed by the surface [Londoño-Calderón et al. 2020]. The peak at 2856 cm^{-1} is related to CH_2 aliphatic hydrocarbons, and the peak at 2924 cm^{-1} shows CH_3 aliphatic hydrocarbons [71]. The peak at 1634 cm^{-1} denotes $\text{C}=\text{C}$ aromatic [Weigel et al. 2017, Marei et al. 2017], and the one at 1385 cm^{-1} represents $\text{C}-\text{H}$ from the methyl group [4]. The peak at 1225 cm^{-1} shows the asymmetric tensile vibration of siloxane groups, according to zeolite Na-ZSM-5 data [Weigel et al. 2017]. The peak at 1085 cm^{-1} also indicates

the asymmetric tension of siloxane groups or S=O sulfoxides [Weigel et al. 2017], while that at 790 cm^{-1} shows poly-aromatic [Marei et al. 2017] and symmetric tension of the siloxane group. Peaks at 674 , 540 , and 468 cm^{-1} imply NiO [Essam et al. 2019, Haider et al. 2019], and the one at 1792 cm^{-1} is related to the carbonyl group C=O [Weigel et al. 2017, Marei et al. 2017].

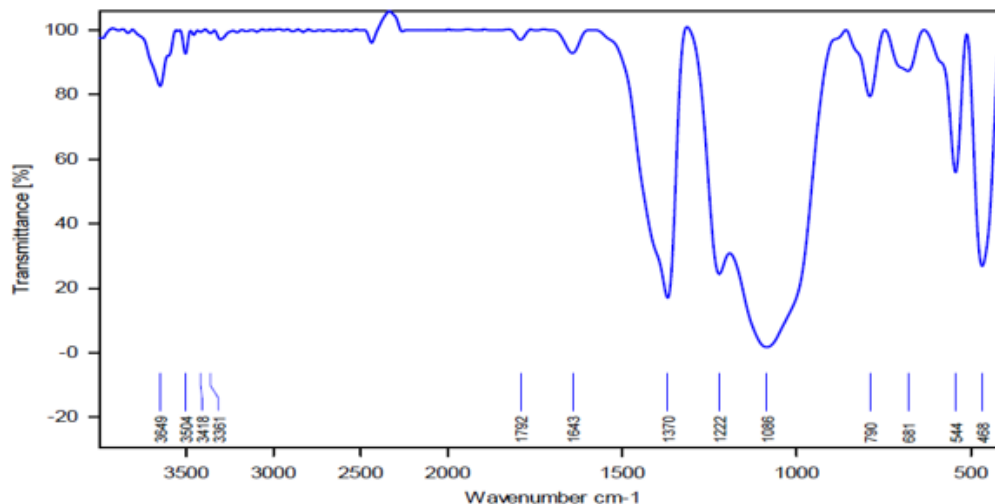


Figure 5

The FTIR spectrum of nickel oxide zeolite Na-ZSM-5.

Considering the nickel peaks, it can be concluded that the catalyst is adequately synthesized. Figure 6 shows the FTIR spectrum of NiO-Na-ZSM-5 zeolite. In addition, comparing Figures 5 with 6 shows that an amount of asphaltene is adsorbed by the catalyst.

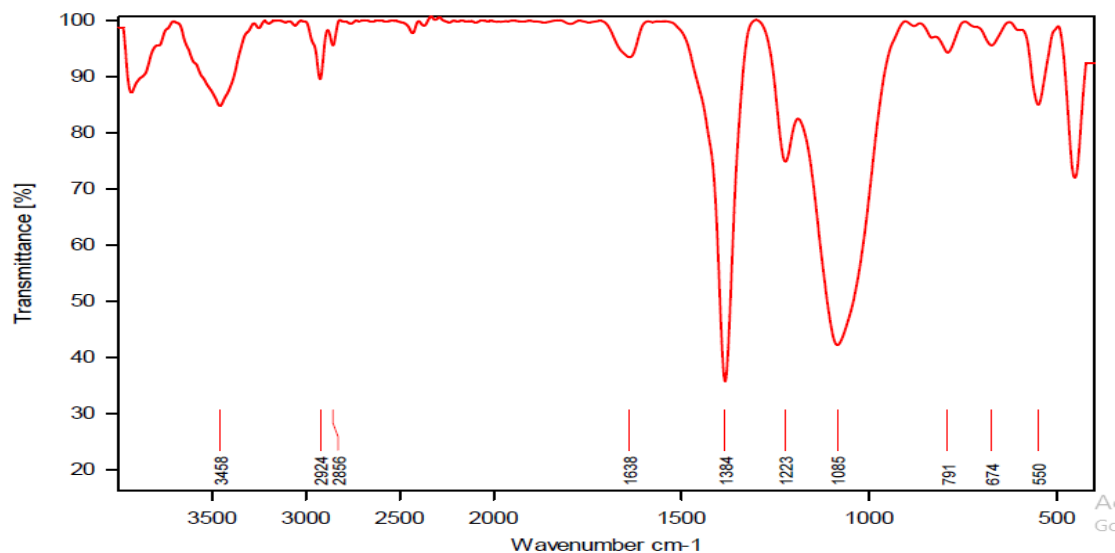


Figure 6

The FTIR spectrum of NiO-Na-ZSM-5 zeolite.

3.4. Morphology of nanoparticles

Figure 7 indicates the SEM images obtained from zeolite Na-ZSM-5 nickel oxide. The catalyst is adequately synthesized, and the nickel particles are observable on the zeolite. Concerning morphology, the zeolite sample comprises numerous coffin-shaped units, which show its crystalline structure. The images show that the synthesized porous combination has an uneven, rough, and riveted surface, which

improves the performance of the catalyst with an approximate size of 13.6 nm. Images are shown from 10 μm to 200 nm. A particle size distribution histogram determined from the SEM images shows a slight variation in the particle size, and the particles are in the range of 4–24 nm, with an average diameter size of 13.6 nm.

3.5. EDXS analysis

The EDXS analysis is carried out to identify existing elements in the catalyst, and the obtained results before and after asphaltene adsorption are presented in Figures 8 and 9.

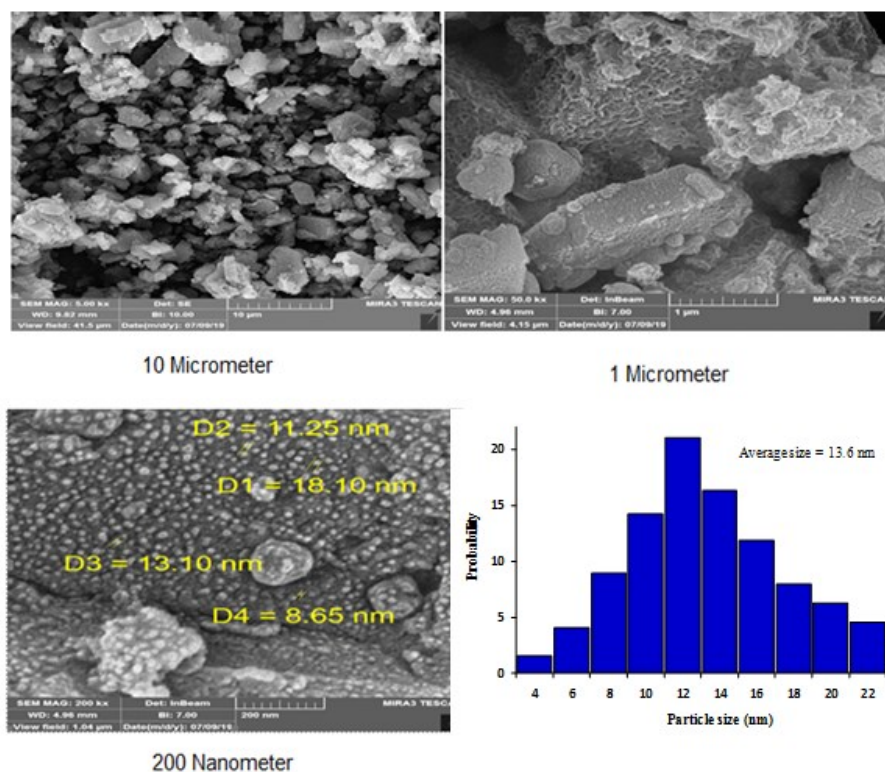
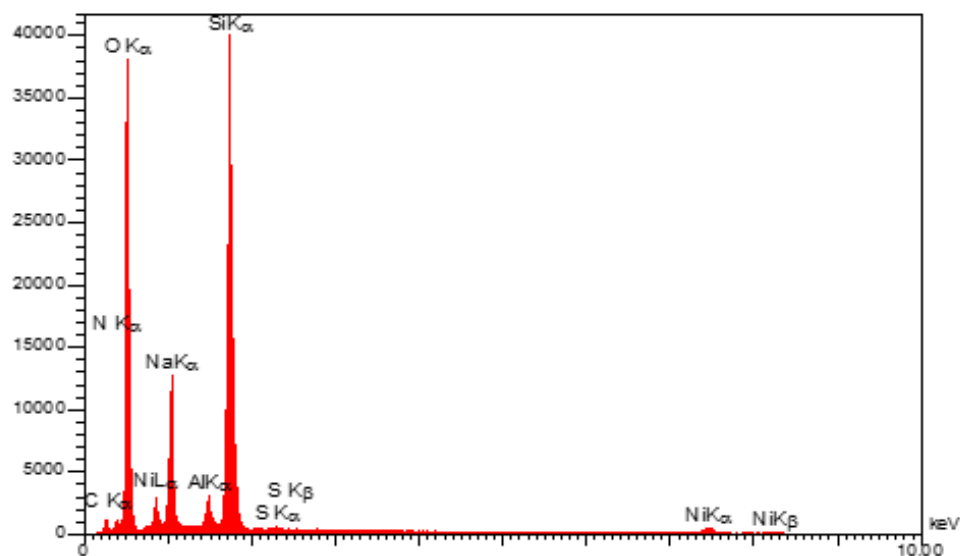
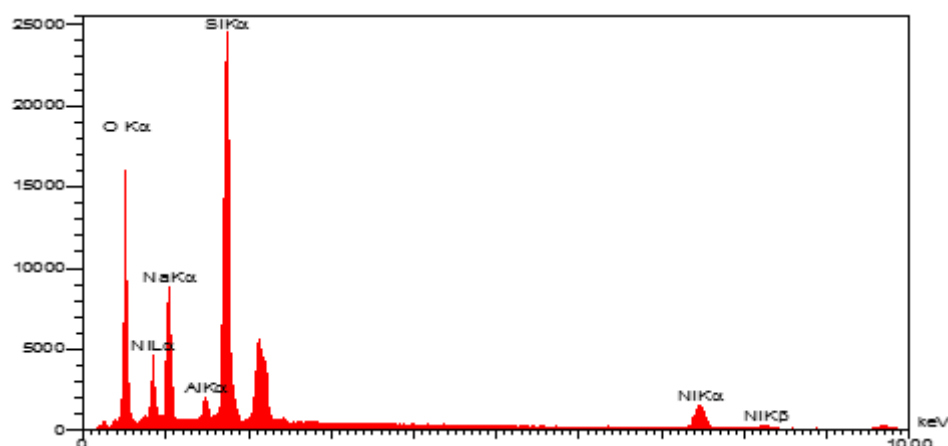


Figure 7

The SEM images of Na-ZSM-5 nickel oxide on 10 μm , 1 μm , and 20 nm scales and its particle size distribution.

**Figure 8**

The EDXS analysis of Na-ZSM-5 nickel oxide before asphaltene adsorption.

**Figure 9**

The EDXS analysis of Na-ZSM-5 nickel oxide after asphaltene adsorption.

The observed peaks are related to Si, Al, Ni, O, and Na, which indicate the absence of impurities in the catalyst. It is observed that the weight of nickel existing in the synthesized catalyst is equal to 4.99%, which differs from the 20% stoichiometry. In addition, the rate of adsorbed asphaltene is shown with the following elements: S = 0.78%, N = 2.63%, and C = 4.62%; this finding indicates the low adsorption rate of asphaltene.

3.6. Evaluating the effect of different parameters on asphaltene adsorption

a. The effect of initial asphaltene concentration

Experiments were carried out (Figures 10–12) with the initial asphaltene concentration of 25–2000 mg/L at a contact time of 2–3 h and a temperature of 25 °C to evaluate the effect of the initial concentration of asphaltene. Then, the same conditions were repeated at a temperature of 40 and 50 °C.

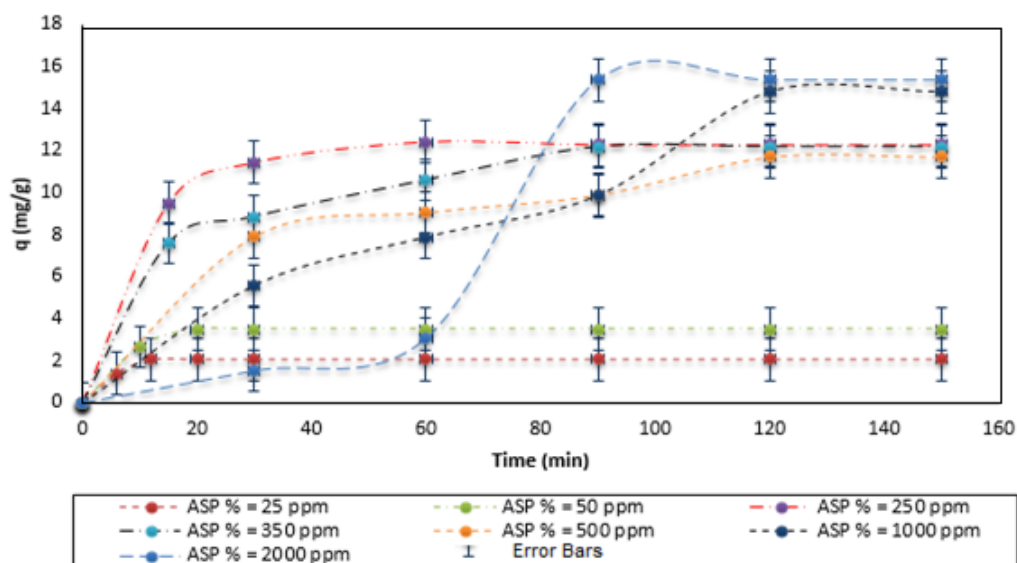


Figure 10

The adsorption graph at different concentrations of asphaltene and 25 °C.

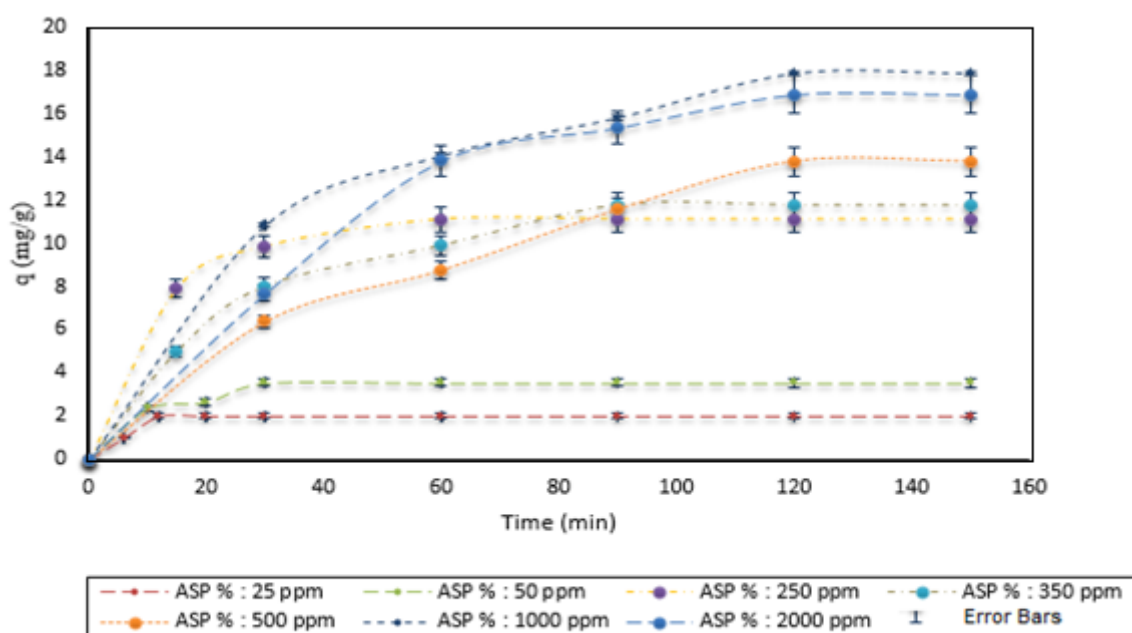


Figure 11

The adsorption graph at different concentrations of asphaltene and 40 °C.

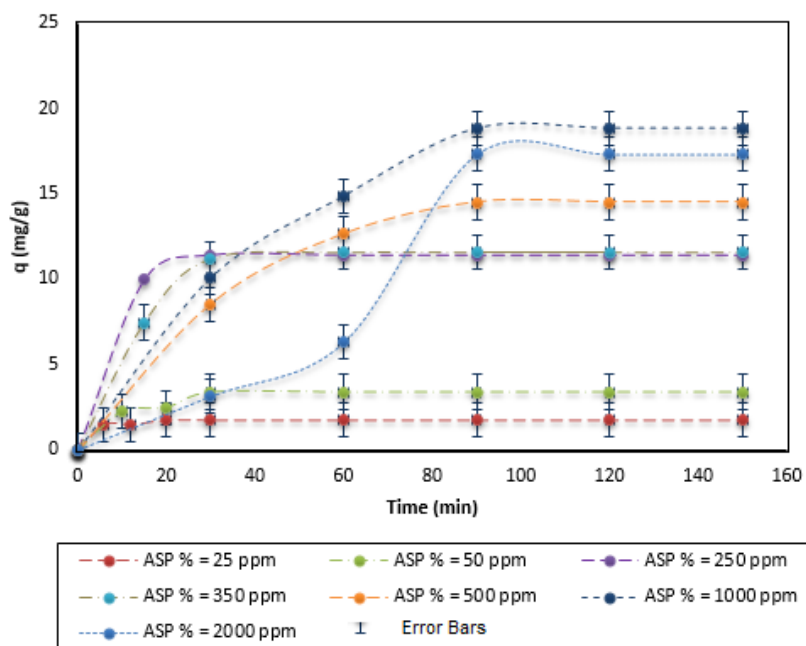


Figure 12

The adsorption graph at different concentrations of asphaltene and 55 °C.

The results indicate that the asphaltene adsorption rate in zeolite increases with an increase in the initial asphaltene concentration from 25 to 2000 ppm. It can be concluded that the initial asphaltene concentration has a considerable effect on the asphaltene adsorption rate. In addition, it is observed from the diagrams that the adsorbent is saturated in less than 2 h and reaches its equilibrium adsorption capacity [Nassar et al. 2010]. From the fact that the adsorbent is saturated in a short period, it can be concluded that surface adsorption is significant, and the permeation phase does not exist in this adsorbent [Nassar et al. 2010].

With an increase in asphaltene concentration, the probability of molecules occupying the adsorbent surface will increase, and thus the adsorption rate will intensify. However, this increase in adsorption rate will continue to a certain extent because at a high asphaltene concentration, almost all adsorption positions are occupied; hence, increasing the initial concentration of asphaltene will not affect the adsorption rate.

The results of asphaltene surface adsorption experiments on the adsorbent at various temperatures are evaluated in the following tables. This evaluation shows that at different temperatures, increasing asphaltene concentration results in increased adsorption on the adsorbent. It can be inferred from these diagrams that the adsorbent is saturated after 2 h and reaches its equilibrium adsorption capacity [30, 40, 75]. For example, 25 ppm of the experimental equilibrium adsorption rate (q_e) equals 2.083333 mg/g. When the concentration increases to 2000 ppm, this amount reaches 15.38462 mg/g.

b. The effect of temperature

The effect of temperature on asphaltene adsorption by zeolite ZSM-5 was studied at 25, 40, and 55 °C with an initial asphaltene concentration of 25–2000 mg/L, an adsorbent dose of 10 g/L, and a contact time of 3 h, as depicted in Figure 13.

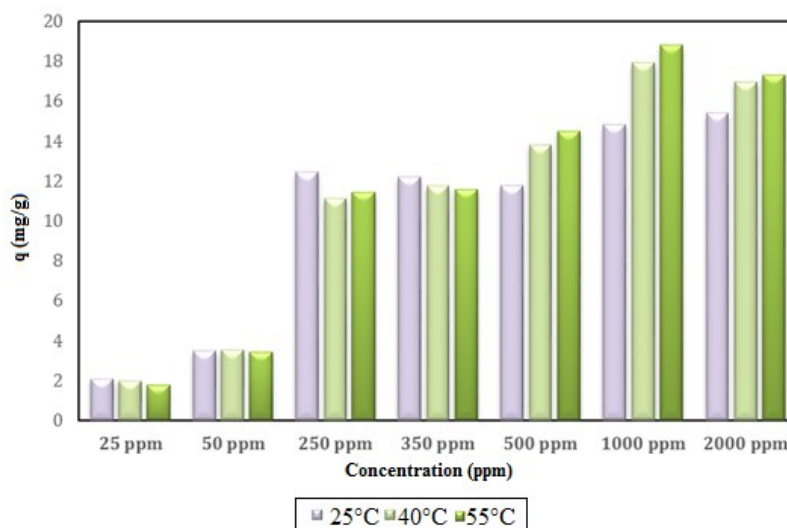


Figure 13

The effect of temperature on the asphaltene adsorption by zeolite ZSM-5.

Numerous studies indicate that increasing temperature in adsorbents such as silica, alumina, and alumina silicate (in which Na-ZSM-5 has a silica-to-alumina ratio of 40 to 1) results in increased asphaltene adsorption on the adsorbent [Gorbaty et al. 2001]. According to Figure 14, the results indicate that at concentrations less than 500 ppm, a rise in the temperature results in reduced asphaltene adsorption, while at concentrations higher than 500 ppm, with a rise in the temperature from 25 to 55 °C, asphaltene adsorption capacity on zeolite increases. Moreover, viscosity decreases, and the dispersion rate increases with an increase in the temperature. At concentrations higher than 500 ppm, increasing temperature can enhance adsorption by breaking the bond between accumulated asphaltenes. Therefore, active surfaces that have been covered inside the entire structure will become visible, and this disintegration of asphaltene aggregation will cause asphaltene agglomeration to become smaller, having higher dispersion rates and enhancing adsorption [Adams et al. 2014]. Thus, it can be concluded that higher temperatures at higher concentrations result in facilitated asphaltene adsorption in the zeolite.

c. The ratio of n-heptane to toluene

n-heptane is an adequate precipitator for asphaltene that has been chosen as the type of solvent effective in asphaltene adsorption. This experiment was evaluated with changes in the H/T from 0 to 0.5, as shown in Figure 14.

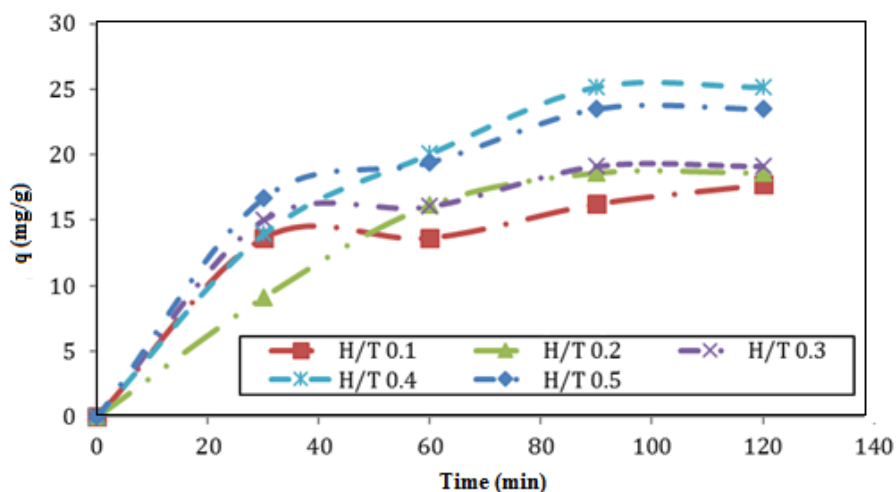


Figure 14

The asphaltene adsorption at different heptane-to-toluene ratios.

An H/T of 0.50 did not improve asphaltene adsorption because increasing H/T to above 0.50 results in asphaltene deposition when the other variables are constant; thus, the adsorption rate is reduced. As shown, with an increase in H/T, the asphaltene adsorption increases, which can be attributed to a reduction in asphaltene solubility, resulting in increased asphaltene aggregation and hence increased adsorption [Alboudwarej et al. 2005]. All the experiments were conducted at a concentration of 1000 ppm and at ambient temperature, and the most significant adsorption was observed for an H/T of 0.4 with $q = 25.17$ mg/g.

d. Reusability behavior of NiO/Na-ZSm-5 for asphaltene adsorption

Figure 15 shows the reusability tests of NiO/Na-ZSm-5 adsorbent in the asphaltene adsorption during four-cycle experiments under the following conditions: asphaltene concentration of 1000 ppm, an H/T of 0.4, and ambient temperature. The adsorbent was washed with distilled toluene and then dried at 60 °C for 5 h. Afterward, it was used in a new experiment after each adsorption assay. As shown in Figure 15, the asphaltene adsorption capacity (q) for the four successive cycles of NiO/Na-ZSm-5 is 25.17, 24.72, 23.91, and 23.36 mg/g. The slight decrease in the asphaltene adsorption activity after four cycles is due to the loss of the adsorbent through washing. The results show that NiO/Na-ZSm-5 is a reusable adsorbent for asphaltene adsorption.

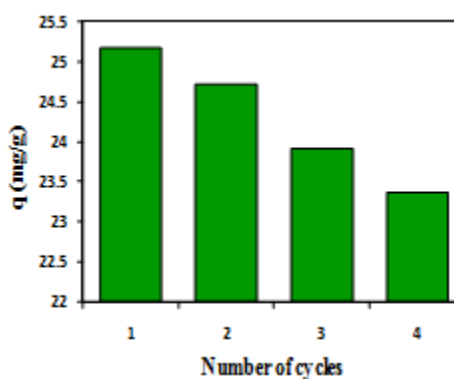


Figure 15

The reusability behavior of NiO/Na-ZSm-5 for asphaltene adsorption.

f. Adsorption isotherm

Studying the equilibrium behavior of the adsorbent is necessary for the design and optimization of adsorption systems. In this study, adsorption of isotherms for all samples was carried out using the Langmuir and Freundlich models. The Langmuir adsorption isotherm assumes monolayer adsorption (the adsorbed asphaltene layer is one molecule in thickness); adsorption only occurs at a finite (fixed) number of definite localized sites that are identical with no lateral interaction between the adsorbed molecules. In its derivation, the Langmuir isotherm refers to homogeneous adsorption, in which each molecule possesses constant enthalpies and sorption activation energy; all sites on NiO/ZSM-5 nanocomposites possess an equal affinity for the adsorbate. Graphically, it is characterized by a plateau, an equilibrium saturation point where no further adsorption can occur once a molecule occupies a site. Moreover, Langmuir's theory has related the rapid decrease of the attractive intermolecular forces to the rise of distance. The following equation represents the Langmuir isotherm model:

$$q_e = \left(\frac{q_m K C_e}{1 + K C_e} \right) \quad (2)$$

where q_e is the amount of asphaltene adsorbed on nanoparticles (mg/g), K indicates Langmuir equilibrium adsorption constant (L/mg), C_e is the equilibrium concentration of asphaltene, and q_m denotes the maximum amount of asphaltene adsorbed on nanoparticles (mg/g).

Freundlich isotherm is the earliest known equation describing the nonideal and reversible adsorption, not restricted to monolayer formation. This empirical model can be applied to multilayer adsorption, with nonuniform distribution of adsorption heat and affinities over the heterogeneous surface. Freundlich isotherm is widely applied in heterogeneous processes, especially for organic compounds or highly interactive species on polar porous media. The following equation represents the Freundlich isotherm model:

$$q_e = K_f (C_e)^{\frac{1}{n}} \quad (3)$$

where K_f is the Freundlich constant ((mg/g)(L/mg) $^{1/n}$), and $1/n$ indicates the adsorption intensity factor (the strength of adsorption or the adsorption affinity). The constants of isotherm can be calculated by plotting $\ln(q_e)$ versus C_e . To this end, several experiments were conducted with different initial concentrations, an adsorption dose of 10 g/L, a contact time of 3 h, and a temperature of 25 °C, as shown in Figures 16 and 17. $1/n$ reveals a heterogeneous level that shows relative energy distribution and heterogeneity of adsorption sites. When $1/n$ is higher than zero ($0 < 1/n < 1$), the adsorption rate is adequate, and when $1/n$ is greater than 1.0, the adsorption process is inadequate. As listed in Table 3, $1/n$ for all the experiments are smaller than 1.0, which shows that the adsorption process is adequate [81].

Table 3
Langmuir and Freundlich parameters constant.

55 °C	40 °C	25 °C	Parameters	Isotherm
18.38	17.76	15.77	q_m	Langmuir $C_e/q_e = 1/K q_m + C_e/q_m$
0.013	0.014	0.017	K	
0.99	0.99	0.99	R^2	

0.970931	1.27	1.51	K_f	Freundlich $\ln(q_e) = \ln(K_f) + 1/n \ln(C_e)$
0.4352	0.39	0.35	$1/n$	
0.92	0.95	0.91	R^2	

In addition, comparing the results obtained from the R^2 demonstrates that the Langmuir model provides a more desirable output than the Freundlich model, implying that asphaltene adsorption by nickel oxide zeolite Na-ZSM-5 occurs at a homogeneous level with a single-layered coating (nature), with uniform distribution from adsorption sites [Ayawei et al. 2017].

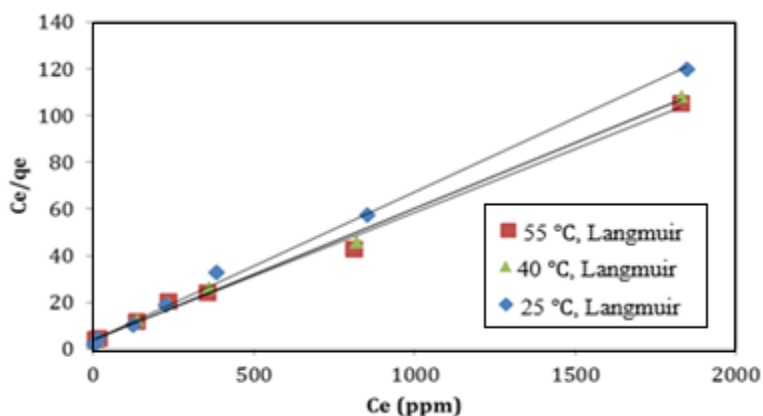


Figure 16

The linear Langmuir constant at different temperatures.

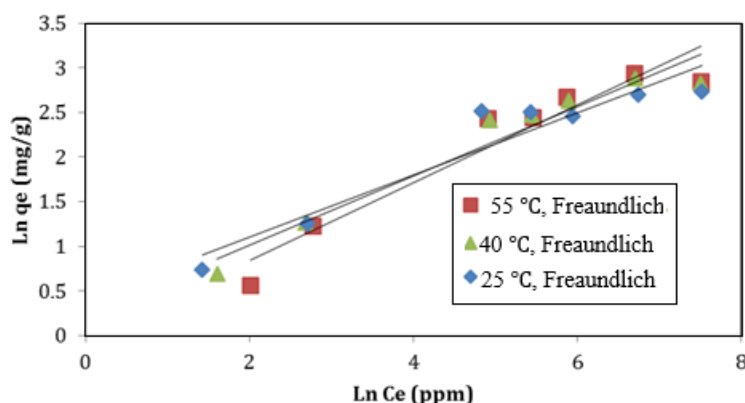


Figure 17

The linear Freundlich constant at different temperatures.

3.7. Evaluating kinetic adsorption models

Synthetic adsorption can be predicted by measuring the rate of asphaltene adsorption by surface nanoparticles of nickel oxide zeolite Na-ZSM-5 at a constant time and temperature. Fitting of the data is conducted with pseudo-first-order and pseudo-second-order linear kinetic equations (Figures 18 and 19). The proof of the pseudo-first-order and pseudo-second-order kinetic equations is calculated and listed in Table 4 using the slope and line's intercept.

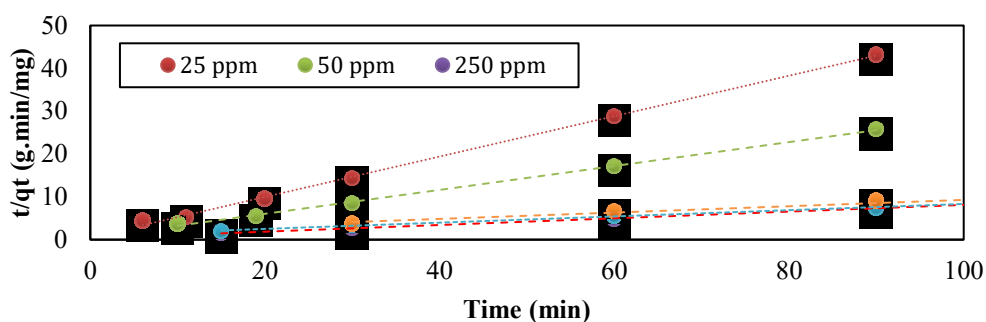


Figure 18

The pseudo-second-order linear kinetic equations for nickel oxide zeolite Na-ZSM-5.

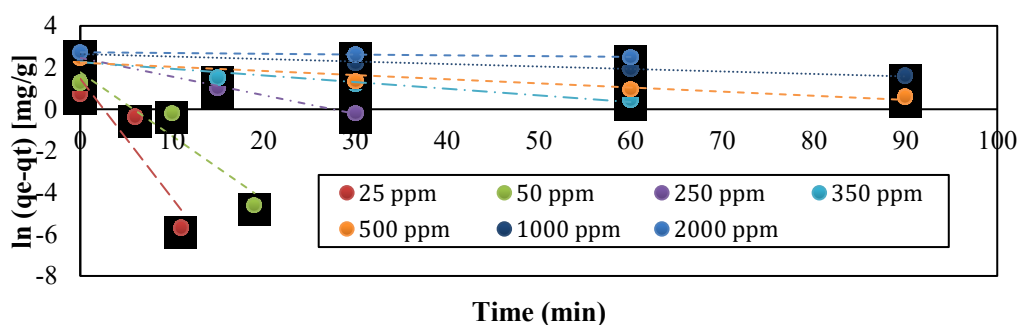


Figure 19

The pseudo-first-order linear kinetic equations for nickel oxide zeolite Na-ZSM-5.

Table 4

The pseudo-first-order and pseudo-second-order linear kinetic parameters for nickel oxide zeolite Na-ZSM-5.

Initial concentrat ion (mg/L	q_e (Experimen tal) (mg/g)	Pseudo-first-order $Ln(q_e - q_t) = Ln(q_e) - K_1 t$			Pseudo-second-order $\frac{t}{q_t} = \frac{1}{K_2 q_e^2} + \frac{t}{q_e}$		
		K_1	R^2	q_e (mg/g)	K_2	R^2	q_e (mg/g)
25	2.083	0.572	0.837	4.319	0.413	0.999	2.119
50	3.5	0.305	0.903	5.887	0.169	0.999	3.582
250	12.43	0.089	0.997	11.735	0.021	0.999	12.771
350	12.194	0.032	0.931	9.571	0.005	0.996	13.755
500	11.716	0.02	0.911	9.337	0.003	0.991	13.532
1000	14.803	0.011	0.988	14.132	0.0002	0.782	29.851
2000	15.384	0.004	0.999	15.415	0.0005	0.566	9.615

The correlation coefficient of fit of data with kinetic equations (R^2) at concentrations of 25 to 500 ppm for the pseudo-second-order kinetic adsorption of asphaltene is exceptionally close to one. It is close to the pseudo-first-order kinetic adsorption at concentrations of 1000 and 2000 ppm. With an increase in the initial concentration of asphaltene, the correlation of the experimental data with the pseudo-second-order kinetic model is reduced, while it matches the pseudo-first-order model. The results show that when the initial concentration is low, the pseudo-second-order model is adequate for adsorption kinetic

analysis, while when the initial concentration of asphaltene is high, the pseudo-first-order model is desirable [Azizian et al. 2004, Ezzati et al. 2020].

When asphaltene adsorption by surface nanoparticles of nickel oxide zeolite Na-ZSM-5 follows the pseudo-second-order adsorption kinetic, there is a reaction between the adsorbent and the adsorbent surface, the rate of which controls the asphaltene surface adsorption process. This can be a reason for eliminating the infiltration step at low adsorption concentrations, resulting in reduced equilibrium time. When the concentration increases, it is compatible with the pseudo-first-order adsorption kinetics, which shows that the infiltration step exists during adsorption at higher concentrations [Azizian et al. 2004].

3.8. Thermodynamic parameters

Thermodynamic features have a significant effect on determining the spontaneity of the adsorption process. Thermodynamic parameter values such as enthalpy changes (ΔH_{ads}) and entropy changes (ΔS_{ads}) should be considered for determining changes in Gibbs free energy (ΔG_{ads}). If the value of ΔG at a definite temperature is negative, the reaction will occur spontaneously [Saha et al. 2011].

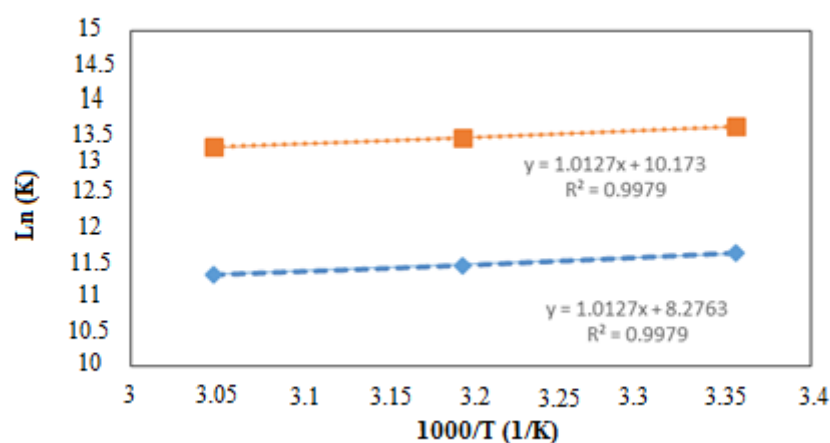
The enthalpy value of the adsorption process is calculated using the Equations (4)–(6):

$$\Delta G^0 = \Delta H^0 - T\Delta S^0 \quad (4)$$

$$\Delta G_{ads}^0 = -RT \ln(K) \quad (5)$$

$$\ln(K) = -\frac{\Delta H_{ads}^0}{RT} + \frac{\Delta S_{ads}^0}{R} \quad (6)$$

where T is the temperature in Kelvin, R indicates the universal gas constant equal to 8.314 J/mol·K, and K is equilibrium balance adsorption (without dimension). The thermodynamic proof can be estimated based on the Langmuir isotherm model. We can use Equation (2) to directly calculate ΔG by linearly plotting $\ln(K)$ versus T^{-1} in Equation (3); by using the slope and width from intercept, ΔS and ΔH values can be calculated, respectively [Adelodun et al. 2016]. The K value can be shown as $K_L C_S$ in which K_L is the Langmuir adsorption isotherm constant (L/mmol), and C_S is the toluene solvent molar concentration in (mmol/L). While K_L is calculated based on liter per milligram, it is necessary to know the molecular weight of asphaltene to convert it to a liter per millimoles. Even though the exact molecular weight of asphaltene is still under investigation, the average molecular weight of asphaltene at 5000 g/mol and 750 reported from various sources are used for the calculations [30, 75]. The thermodynamic parameter values for asphaltene adsorption on zeolite Na-ZSM-5 are presented in Figure 20. For both molecular weights of asphaltene at all temperatures, ΔH_{ads} values were negative, indicating that the adsorption process is an exothermic reaction.

**Figure 20**

Changes in $\ln(K)$ versus $1/T$ for asphaltene adsorption on zeolite Na-ZSM-5 nickel oxide.

The dependence of the adsorbent on the adsorbed material is expressed as a positive value of ΔS , which shows the increase in random collisions [Saha et al. 2011]. In addition, the positive values of changes in entropy indicate that random collisions increase with asphaltene adsorption on the nickel oxide Na-ZSM-5 adsorbent [47].

Table 5 lists calculated thermodynamic values for asphaltene adsorption in the presence of nickel oxide Na-ZSM-5. Changes in Gibbs free energy (ΔG_{ads}) for the adsorbent were negative for all the temperatures [84]. An increase in the negative value of Gibbs free energy along with an increase in the temperature shows that the process is more efficient at higher temperatures [Tan et al. 2014]. Furthermore, it indicates that the degree of spontaneity at higher temperatures is enhanced [Vijayakumar et al. 2012].

Table 5

Thermodynamic values for asphaltene adsorption in the presence of nickel oxide Na-ZSM-5.

Asphaltene molecular weight (g/mol)	T (K)	$-\Delta G_{ads}$ (kJ/mol)	$-\Delta H_{ads}$ (kJ/mol)	ΔS_{ads} (J/mol.K)	R^2
750	298	28.934	8.419	68.809	0.998
	313	29.935			
	328	31.001			
5000	298	33.634	8.419	84.578	0.998
	313	34.872			
	328	36.174			

4. Conclusions

This research employed zeolite–nickel oxide nanoparticles as asphaltene absorbers and confirmed their ability to adsorb asphaltene molecules using EDXS and UV tests. Based on the kinetic adsorption models in the presence of nanoparticles, when the initial concentration of asphaltene is low, the pseudo-second-order model is appropriate for the kinetic analysis of adsorption. The pseudo-first-order model is adequate when the initial asphaltene concentration is high. Raising the initial concentration of asphaltene increases adsorption due to the higher concentration gradient between the asphaltene solvent

and adsorbent. Moreover, when the temperature increases from 25 to 55 °C, the asphaltene adsorption capacity on the sorbent rises. The Langmuir model has a more suitable outcome than the Freundlich model, which indicates that asphaltene adsorption by the adsorbent has a single-layer essence with uniform distribution from adsorption sites. Based on surveying thermodynamic properties at the last steps, it was concluded that for all the samples at different temperatures, the ΔH values were negative, demonstrating that the adsorption process is pyrogenic. Furthermore, changes in Gibbs free energy for the adsorbent at all temperatures were negative, which implies the spontaneity of the asphaltene adsorption process.

Nomenclature

C_e	Equilibrium sorption of asphaltene (mg/g)
EDXS	Energy-dispersive X-ray spectroscopy
FTIR	Fourier-transform infrared spectroscopy
H/T	Heptane-to-toluene ratio
K_1	First-order kinetic constant (1/min)
K_2	Second-order kinetic constant (g/mg.min)
K_f	Asphaltene adsorption capacity factor ((mg/g) (L/mg)) ^{1/n})
K_L	The Langmuir equilibrium (L/mg)
q_e	Asphaltene absorption in equilibrium time (mg/g)
q_m	Maximum adsorption capacity of the activated carbon (mg/g)
q_t	Asphaltene absorption in equilibrium time t (mg/g)
SARA	Saturates, aromatics, resins, and asphaltenes
SEM	Scanning electron microscopy
XRD	X-ray diffraction
ΔH_{ads}	Enthalpy changes
ΔS_{ads}	Entropy changes
ΔG_{ads}	Gibbs free energy change

References

- Acevedo, S., Ranaudo, M. A., García, C., Castillo, J., & Fernández, A., Adsorption of Asphaltenes at The Toluene–silica Interface: A Kinetic Study, *Energy & Fuels*, Vol.17, p.257-261, 2003
- Acevedo, S., Ranaudo, M. A., García, C., Castillo, J., Fernández, A., Caetano, M., & Goncalvez, S., Importance of Asphaltene Aggregation in Solution in Determining the Adsorption of This Sample on Mineral Surfaces. *Colloids and Surfaces A: Physicochemical and Engineering Aspects*, Vol.166, p.145–152, 2000,
- Adams, J.J., Asphaltene Adsorption, a Literature Review. *Energy and Fuels*, Vol.28, p.2831–2856, 2014,
- Adelodun, A. A., Ngila, J. C., Do-Gun Kim, Young-Min Jo., Isotherm, Thermodynamic and Kinetic Studies of Selective CO₂ Adsorption on Chemically Modified Carbon Surfaces. *Aerosol and Air Quality Research*, Vol.16, p.3312–3329, 2016.
- Alboudwarej, H., Pole, D., Svrcek, W. Y., & Yarranton, H. W., Adsorption of Asphaltenes on Metals, *Industrial & Engineering Chemistry Research*, Vol.44, p.5585–592, 2005.

- ASTM D6560-17, Standard Test Method for Determination of Asphaltenes (Heptane Insolubles) in Crude Petroleum and Petroleum Products, ASTM International, West Conshohocken, PA, [Www.Astm.Org](http://www.Astm.Org), 2005, 2017.
- Ayawei, N., Ebelegi, A. And Wankasi, D., Modelling and Interpretation of Adsorption Isotherms. *Journal of Chemistry*, p.1-11, 2017.
- Azizian, S., Kinetic Models of Sorption: A Theoretical Analysis. *Journal of Colloid and Interface Science*, Vol.276, p.47–52, 2004.
- Bahraminejad, H., Manshad, A. K., Riazi, M., Ali, J.A., Sajadi, S.M., Keshavarz, A., CuO/TiO₂/PAM As a Novel Introduced Hybrid Agent for Water—Oil Interfacial Tension and Wettability Optimization in Chemical Enhanced Oil Recovery, *Energy Fuels*, Vol.33, No.11, p.10547–10560, <https://doi.org/10.1021/acs.energyfuels.9b02109>, 2019.
- Balabin R. M., Safieva R. Z. And Lomakina E. I., Gasoline Classification Using Near Infrared (NIR) Spectroscopy Data: Comparison of Multivariate Techniques, *Analytica Chimica Acta*, Vol.671, p.27–35, 2010.
- Belal, J. Abu., and Tarboush, M. M. H., Adsorption of Asphaltenes from Heavy Oil onto in Situ Prepared NiO Nanoparticles. *Journal of Colloid and Interface Science*, Vol.378, p.64-69, 2012.
- Bouhadda, Y., Bormann, D., Sheu, E., Bendedouch, D., Krallafa A., and Daaou, M., Characterization of Algerian Hassi-Messaoud Asphaltene Structure Using Raman Spectrometry and X-Ray Diffraction. *Fuel*, Vol.12, p.1855-1864, 2007.
- Camilo Franco, E. P., Benjumea, P., Marco, A., Ruiz, And Farid B., Cortés., Kinetic and Thermodynamic Equilibrium of Asphaltenes Sorption onto Nanoparticles of Nickel Oxide Supported on Nanoparticulated Alumina, *Fuel*, Vol.105, p.408-414, 2013.
- Charchi Aghdam, N., Ejtemaei, M., Sharafi, S. M., Babaluo, A. A., Tavakoli, A., Bayati, B., Catalytic Performance of Nanostructured Pt/ZSM-5 Catalysts Synthesized by Extended Charnell's Method in Hydroisomerization of N-Pentane, *Polyhedron*, Vol.162, p.155–164, 2019.
- Cortés, F.B., Mejía, J.M., Ruiz, M.A., Benjumea, P., and Riffel, D.B., Sorption of Asphaltenes onto Nanoparticles of Nickel Oxide Supported on Nanoparticulated Silica Gel, *Energy & Fuels*, Vol. 26, p.1725–1730, 2012.
- De Oliveira, T.K.R., Rosset, M., Perez-Lopez, O.W., Ethanol Dehydration to Diethyl Ether Over Cu-Fe/ZSM-5 Catalysts, *Catal. Commun.*, Vol.104, p.32–36, 2018.
- Dong, H., Xia, M., Wang, C., Li, G., & Luo, Y., Al/NiO Nanocomposites for Enhanced Energetic Properties: Preparation by Polymer Assembly Method. *Materials & Design*, Vol.183, 108111P., 2019.
- Escobedo, J. And Mansoori, G. A., Heavy-Organic Particle Deposition from Petroleum Fluid Flow in Oil Wellsand Pipelines. *Petroleum Science*, Vol. 7, p.502-508, 2010.
- Eslahati, M., Mehrabianfar, P., Akbarisar, A., Bahraminejad, A., Manshad, A. K., Keshavarz, A., Experimental Investigation of Alfalfa Natural Surfactant and Synergistic Effects Of Ca²⁺, Mg²⁺, And SO₄²⁻ Ions for EOR Applications: Interfacial Tension Optimization, Wettability Alteration And imbibition Studies, *Journal of Molecular Liquids*, Vol.310, 113123P., 2020.

- Ezzati, R., Derivation of Pseudo-first-order, Pseudo-second-Order and Modified Pseudo-first-order Rate Equations from Langmuir and Freundlich Isotherms for Adsorption, *Chemical Engineering Journal*, Vol.392, p.123705, 2020.
- Fakeeha, A.H., Al-Fatesh, A.S., Abasaeed, A.E., Stabilities of Zeolite-supported Ni Catalysts for Dry Reforming of Methane. *Chin. J. Catal*, Vol.34, p.764–768, 2013.
- Ferworn, K. A., Svrcek, W. Y., And Mehrotra A. K., Measurement of Asphaltene Particle Size Distributions in Crude Oils Diluted With N-Heptane, *Ind. Eng. Chem. Res*, Vo.32, p.955-959, 1993.
- Franco C.A., Influence of Asphaltene Aggregation on The Adsorption and Catalytic Behavior of Nanoparticles, *Energy Fuels*29, p.1610–1621, 2015.
- Franco, C. A., J., Giraldo, M. A., Ruiz, B. A., Rojano and Cortes, F. B., Kinetic and Thermodynamic Equilibrium of Asphaltenes Sorption onto Formation Rock: Evaluation of The Wash in The Adsorptive Properties, *Dyna*, Vol.176, p.81-89, 2012.
- Freundlich, H. M. F., Over the Adsorption in Solution, *J. Phys. Chem*, Vol.57, p.385–471, 1906.
- Gorbaty, M. L.; Errughelli, T. T.; Olmstead, W. N.; Miseo, S.; Soled, S. L.; Robbins, W. K. Selective Adsorption Process for Resid Upgrading. US Patent 6245223, June 12, 2001.
- González G., Travalloni-Louvisse A. M. And Petrobras S. A., Adsorption of Asphaltenes and Its Effect on Oil Production. *SPE Production & Facilities*, Vol.8, p.91–96, 1993.
- Gonzalez, M. F.; Stull, C. S.; Lopez-Linares, F.; Pereira-Almao, P., Comparing Asphaltene Adsorption with Model Heavy Molecules Over Macro Porous Solid Surfaces. *Energy Fuels*, Vol.21, p.234-241, 2007.
- Groenzin, H. And Mullins O. C., Molecular Size and Structure of Asphaltenes from Various Sources. *Energy & Fuels*3, p.677-684, 2000.
- Hasanvand M. Z., Ahmadi M. A., and Behbahani R. M., Solving Asphaltene Precipitation Issue in Vertical Wells via Redesigning of Production Facilities. *Petroleum*, Vol.1, p.139-145, 2015.
- Hashem, M., Saion, E., Al-Hada, N. M., Kamari, H. M., Shaari, A. H., Talib, Z. A., Kamarudeen, M. A., Fabrication and Characterization of Semiconductor Nickel Oxide (NiO) Nanoparticles Manufactured Using a Facile Thermal Treatment. *Results In Physics*, Vol.6, p.1024–1030, 2016.
- He, Y., Zeolite Supported Fe/Ni Bimetallic Nanoparticles for Simultaneous Removal of Nitrate and Phosphate: Synergistic Effect and Mechanism. *Chemical Engineering Journal*, Vol.347, p.669–681, 2018.
- Hemmati-Sarapardeh, A., Alipour-Yeganeh-Marand, R., Naseri, A., Safiabadi, A., Gharagheizi, F., Ilani-Kashkouli, P., & Mohammadi, A. H., Asphaltene Precipitation Due to Natural Depletion of Reservoir: Determination Using A SARA Fraction Based Intelligent Model. *Fluid Phase Equilibria*, Vol.354, p.177–184, 2013.
- Hosseinpour, N., Asphaltene Adsorption onto Acidic/Basic Metal Oxide Nanoparticles Toward in Situ Upgrading of Reservoir Oils by Nanotechnology. *Langmuir*, Vol.29, p.14135–14146, 2013.
- Hosseinpour, N., Mortazavi, Y., Bahramian, A., Khodatars, L., Khodadadi. A.A., Enhanced Pyrolysis and Oxidation of Asphaltenes Adsorbed onto Transition Metal Oxides Nanoparticles Towards Advanced In-Situ Combustion. *EOR Processes by Nanotechnology, Applied Catalysis A: General*, Vol.477, p.159–171, 2014.

- Jia, N., Memon, A., Gao, J., Zuo, J., Zhao, H., Three-phase Equilibrium Study for Heavy-Oil/Solvent/Steam System at High Temperatures. *J Can Petrol Technol*, Vol.50, p.68–79, 2011.
- Jouault, N., Corvis, Y., Cousin, F., Jestin, J., and Barr, L., Asphaltene Adsorption Mechanisms on The Local Scale Probed by Neutron Reflectivity: Transition from Monolayer to Multilayer Growth Above the Flocculation Threshold. *Langmuir*, Vol.25, p.3991-3998, 2009.
- Kazemzadeh, Y., Eshraghi, S.E., Kazemi, K., Sourani, S., Mehrabi, M., Ahmadi, Y., Behavior of Asphaltene Adsorption onto The Metal Oxide Nanoparticle Surface and Its Effect on Heavy Oil Recovery, *Ind. Eng. Chem. Res*, Vol.54, p.233–239, 2015.
- Khoshandam, A., and Alamdari A., Kinetics of Asphaltene Precipitation in a Heptane-toluene Mixture, *Energy Fuels*, Vol.24, p.1917-1924, 2010.
- Kinitisch, E., Clery, D., Service R.F., Normile, D., Coontz, R., Bohannon, J., Sustainability and Energy, *Science*, Vol.315, p.781–813, 2007.
- Kosinov, N., Liu, C., Hensen, E.J., Pidko, E.A., Engineering of Transition Metal Catalysts Confined in Zeolites. *Chem. Mate*, Vol.30, p.3177–3198, 2018.
- Kralova, I., Sjöblom, J., Øye, G., Simon, S., Grimes, B. A., & Paso, K., Heavy Crude Oils/Particle Stabilized Emulsions. *Advances in Colloid and Interface Science*, Vol.169, p.106–127, 2011.
- Langmuir, I., the Constitution and Fundamentals Properties of Solids and Liquids, Part I. Solids. *J. Am. Chem. Soc*, Vol.38, p.2221–2295, 1916.
- Lei, J., Niu, R., Li, J., & Wang, S., the Pd/Na-ZSM-5 Catalysts with Different Si/Al Ratios on Low Concentration Methane Oxidation. *Solid State Sciences*, Vol.101, p.106097, 2020.
- Leontaritis K. J., And Mansoori G. A., Asphaltene Flocculation during Oil Recovery and Processing: A Thermodynamic Colloidal Model. In *The SPE International Symposium on Oilfield Chemistry*, San Antonio, USA, SPE 16285, 1987.
- Londoño-Calderón, V., Ospina, R., Rodriguez-Pereira, J., Rincón-Ortiz, S. A., Restrepo-Parra, E., Molybdenum and Nickel Nanoparticles Synthesis by Laser Ablation Towards the Preparation of a Hydrodesulfurization Catalyst, *Catalysts*, Vol.10, p.1076. Doi: 10.3390/Catal10091076, 2020
- Ma, X., Sprague, M., And Song, C., Deep Desulfurization of Gasoline by Selective Adsorption Over Nickel-Based Adsorbent for Fuel Cell Applications. *Industrial And Engineering Chemistry Research*, 44, p.5768–5775, 2005.
- Mansoori, A., Remediation of Asphaltene and Other Heavy Organic Deposits in Oil Wells and In Pipelines,” *Proceedings W НАУЧНЫЕ ТРУДЫ*, 2010.
- Mclean, J. D., & Kilpatrick, P. K., Comparison of Precipitation and Extrography in The Fractionation of Crude Oil Residua, *Energy & Fuels*, Vol.11, 570–585,1997.
- Mehrabianfar, P., Bahraminejad, H., Manshad, A. K., an Introductory Investigation of a Polymeric Surfactant from a New Natural Source in Chemical Enhanced Oil Recovery (CEOR). *Journal of Petroleum Science and Engineering*, Vol.198, p.108172, 2021.
- Marczewski A. W. And Szymula M., Adsorption of Asphaltenes from Toluene on Mineral Surface. *Colloids Surf. A: Physicochem. Eng. Aspects*, Vol.208, p.259-266, 2002.
- Marei, N.N.; Nassar, N.N.; Hmoudah, M.; El-Qanni, A.; Vitale, G.; Hassan, A., Nanosize Effects of Nio Nanosorbcat on Adsorption and Catalytic Thermo- Oxidative Decomposition of Vacuum Residue Asphaltenes. *Can. J. Chem. Eng*, Vol.95, p.1864–1874, 2017.

- Marei, N. N., Nassar, N. N., Vitale, G., Hassan, A., Maria Josefina Pérez Zurita., Effects of The Size of Nio Nanoparticles on The Catalytic Oxidation of Quinolin-65 As an Asphaltene Model Compound, *Fuel*, Vol.207, p.423-437, 2017.
- Medina, O.E.; Gallego, J.; Restrepo, L.G.; Cortés, F.B.; Franco, C.A., Influence of The Ce^{4+}/Ce^{3+} Redox-Couple on The Cyclic Regeneration for Adsorptive and Catalytic Performance of Nio-Pdo/Ceo₂±Δ Nanoparticles For N-C7 Asphaltene Steam Gasification. *Nanomaterials*, 2019, 9, 734.
- Mirzayi, B. And Naghdi Shayan, N., Adsorption Kinetics and Catalytic Oxidation of Asphaltene on Synthesized Maghemite Nanoparticles. *Journal of Petroleum Science and Engineering*, 2014, 121, 134-141.
- Mullins, O. C., Betancourt, S. S., Francois, E. C. And Jefferson, X. D., the Colloidal Structure of Crude Oil and the Structure of Oil Reservoirs. *Energy & Fuels*, 2007, 21, 2785-2794.
- Milovanović, J., Rajić, N., Romero, A. A., Li, H., Shih, K., Tschentscher, R., & Luque, R., Insights into The Microwave-Assisted Mild Deconstruction of Lignin Feedstocks Using Nio-Containing ZSM-5 Zeolites. *ACS Sustainable Chemistry & Engineering*, 2016, 4, 4305–4313.
- Mishra AK, Bandyopadhyay S, Das D., Structural and Magnetic Properties of Pristine And Fe-Doped Nio Nanoparticles Synthesized By The Co-Precipitation Method. *Materials Research Bulletin*. 2012, 47, 2288-2293.
- Nassar N. N., Hassan A. And Pereira Almas P., Thermogravimetric Studies Oncatalytic Effect of Metal Oxide Nanoparticles on Asphaltene Pyrolysis Under Inert Conditions. *Thermal Analysis and Calorimetry*, 2011, 110, 1327-1332.
- Nassar, N. N., Franco, C. A., Montoya, T., Cortes, F. B., Hassan, A., Effect of Oxide Support on Ni-Pd Bimetallic Nanocatalysts for Steam Gasification of N-C7 Asphaltenes. *Fuel*, 2015, 156, 110–120.
- Nassar, N. N., Asphaltene Adsorption onto Alumina Nanoparticles: Kinetics and Thermodynamic Studies. *Energy Fuels*, Vol.24, p.4116–4122, 2010.
- Nassar, N. N.; Hassan, A.; Pereira-Almas, P., Metal Oxide Nanoparticles for Asphaltene Adsorption and Oxidation, *Energy & Fuels*, Vol.25, p.1017–1023, 2011.
- Nassar, N.N., Iron Oxide Nanoparticles for Rapid Adsorption and Enhanced Catalytic Oxidation of Thermally Cracked Asphaltenes. *Fuel*, Vol.95, p.257–262, 2012.
- Nazarahari, M.J., Manshad, A.K., Moradi, S., Shafiei, A., Ali, J.A., Sajadi, S.M., Keshavarz, A. Synthesis, Characterization, and Assessment of A Ceo₂@Nanoclay Nanocomposite for Enhanced Oil Recovery, *Nanomaterials*, Vol. 10, No.11, p.2280; <https://doi.org/10.3390/Nano10112280>, 2020.
- Novaki, L.P., Moraes, E.O., Goncalves, A.B., De Lira, R.A., Linhares, V.N., De Oliveira, M.C.K., Meireles, F.A., Gonzalez, G., And El Seoud, O.A., Solvatochromic and Solubility Parameters of Solvents: Equivalence of The Scales and Application to Probe the Solubilization of Asphaltenes. *Energy And Fuels*, Vol.30, p.4644–4652, 2016.
- Nowrouzi, I., Mohammadi, A. H., Manshad, A. K., Characterization and Likelihood Application of Extracted Mucilage From Hollyhocks Plant As A Natural Polymer In Enhanced Oil Recovery Process By Alkali-Surfactant-Polymer (ASP) Slug Injection Into Sandstone Oil Reservoirs. *Journal of Molecular Liquids*, Vol.320, p.114445, 2020.

- Qiao, H., Wei, Z., Yang, H., Zhu, L., & Yan, X., Preparation and Characterization of Nio Nanoparticles by Anodic Arc Plasma Method. *Journal of Nanomaterials*, p.1–5, 2009.
- Östlund, J. A., Wattana, P., Nydén, M., & Fogler, H. S., Characterization of Fractionated Asphaltenes By UV–Vis and NMR Self-diffusion Spectroscopy, *Journal of Colloid and Interface Science*, Vol.271, p.372–380, 2004.
- Raj, G., Larkin, E., Lesimple, A., Commins, P., Whelan, J., & Naumov, P., In Situ Monitoring of The Inhibition of Asphaltene Adsorption by A Surfactant on Carbon Steel Surface. *Energy & Fuels*, Vol.33, p.2030–2036, 2019.
- Rahdar, A., Aliahmad, M., and Azizi, Y., Nio Nanoparticles: Synthesis and Characterization. *Journal of Nanostructures*, 5, p.145–151, 2015.
- Rudyk, S., & Spirov, P., Upgrading and Extraction of Bitumen from Nigerian Tar Sand by Supercritical Carbon Dioxide. *Applied Energy*, Vol.113, p.1397–1404, 2014.
- Saha, P., Chowdhury, Sh., Insight into Adsorption Thermodynamics, Thermodynamics, Prof. Mizutani Tadashi (Ed.), ISBN: 978-953-307-544-0, 2011.
- Sedighi M, Mohammadi M., Application of Green Novel Nio/ZSM-5 for Removal of Lead and Mercury Ions from Aqueous Solution: Investigation of Adsorption Parameters. *J. Water Environ. Nanotechnol*, Vol.3, p.301–310, 2018.
- Tan, J., Wei, X., Ouyang, Y., Fan, J., & Liu, R., Adsorption Properties of Copper (II) Ion from Aqueous Solution by Starch-Grafted Polyacrylamide and Crosslinked Starch-Grafted Polyacrylamide. *Periodica Polytechnica Chemical Engineering*, Vol.58, p.131–139, 2014.
- Shams-Ghahfarokhi, Z., Nezamzadeh-Ejchieh, A., As-Synthesized ZSM-5 Zeolite as a Suitable Support for Increasing the Photoactivity of Semiconductors in a Typical Photodegradation Process. *Materials Sciencein Semiconductor Processing*, 39, 265–275, 2015.
- Simo, S., Barre, L., And Palermo. Relationships between Solution and Interfacial Properties of Asphaltenes Aggregates. Presented As Poster on Molecular Structure of Heavy Oil and Coal Liquefaction Products, Vol.12–13, IFP-Lyon (France), 2007.
- Tu, Y.; Kung, J., Mccracken, T., Kotlyar, L.; Kingston, D.; Sparks, B., Effect of Clay Particle Size on The Adsorption of a Pentane Insoluble Bitumen Fraction. *Clay Science*, Vol.12, p.194–198, 2006.
- Vijayakumar, G., Tamilarasan, R., Dharmendirakumar M., Adsorption, Kinetic, Equilibrium and Thermodynamic Studies on the Removal of Basic Dye Rhodamine-B from Aqueous Solution by the Use of Natural Adsorbent Perlite. *J. Mater. Environ. Sci.*, Vol.3, p.157–170, 2012.
- Weigel, S., & Stephan, D., The Prediction of Bitumen Properties based on FTIR And Multivariate Analysis Methods, *Fuel*, Vol.208, p.655–661, 2017.
- Yudin, I. K., Nikolaenko, G. L., Gorodetskii, E. E., Mechanisms of Asphaltene Aggregation in Toluene–Heptane Mixtures, *Journal of Petroleum Science and Engineering*, Vol.20, p.297–301, 1998.
- Zhang, D., Creek, J., Jamaluddin, A.J., Marshall, A.G., Rodgers, R.P., Mullins, O.C., Asphaltenes Problematic but Rich in Potential, *Oilf. Rev*, Vol.19, 22–43, 2007.
- Ziebro, J., Łukasiewicz, I., Borowiak-Palen, E., Michalkiewicz, B., Low Temperature Growth of Carbon Nanotubes from Methane Catalytic Decomposition Over Nickel Supported on A Zeolite, *Nanotechnology*, Vol.21, 145308. Doi:10.1088/0957-4484/21/14/145308, 2010.